The Effect of Constructing Two Adjacent Bridges on the Flow Characteristics and Local Scour around Bridge Piers

Magdy H. Mowafy and Maha R. Fahmy

Water Engineering Dept., Faculty of Engineering, Zagazig University, Egypt

Abstract

Due to the extension of crowded old cities, across have canals and drains, such as Zagazig and banha, the cities' council decided to construct new bridges beside the old one. The distance between the old and new bridges is very small. The main objectives of this research are studying the effect of constructing a new bridge, beside an old one, on the flow characteristics and local scour around piers. The optimum distance between the two bridges which prevents the effect of the second bridge piers on the first one will be studied. An experimental work was conducted in an open channel flume in Water Engineering Lab., Zagazig University. Two different piers shape were tested at space between upstream and downstream piers equal 0.0, 0.5D, D, 2D, 4D, 8D, 16D, and 32D. Four cases were tested, the first is two rectangular piers in upstream and downstream, the second is two circular piers in upstream and downstream, the third is circular pier in upstream with rectangular pier in downstream, and the final case is rectangular pier in the upstream with circular pier in downstream.

Introduction

Scour is defined as the removal of movable bed materials due to erosive action of water. Local scour decreases the bed level at obstruction along the waterway. There were many empirical formulae developed due to experimental work and field study to estimate local scour around piers but no one studied the effect of constructing new piers in upstream or downstream the existing pier.

Farhoud, J. and Smith, K. V. H. (1982) studied experimentally time scale for scour downstream of hydraulic structures. Chiew, Y. M. and Melville, B. W. (1987) developed three empirical functions to estimate scour depth as a function of the approach velocity, sediment size, and flow depth. Uyumaz, A. (1988), investigated experimentally the scour phenomenon in noncohesive soils below the vertical gates for simultaneous flow over and under gate. Melville, B. W. and Sutherland, A. J., (1989) designed a new method to estimate the local scour around piers depending on the wide variation of the experimental data. Mason, P. J. (1989) studied experimentally the effects of air entertainment on plunge pool scour. He developed different empirical formulae used to estimate the scour depth taking the effect of aeration into consideration. Chiew, Y. M. (1992) discussed the protection of piers from scour using riprap material. Kothyari, U. C. et al. (1992) studied the process of scour around circular piers. They developed an equation to estimate the scour depth during live bed scour. Johnson, P. A. (1995) compared between results of pier scour equation and the field data. Chiew, Y. M. (1995) investigated experimentally the stability of riprap layer around cylindrical piers. Melville, B. W. and Raudkivi, A. J. (1996) investigated experimentally the effects of foundation geometry on pier scour. They developed different design relationship for three cases of study, the floor under the bed, the floor within the bed, the floor above the bed. Melville, B. W. (1997) presented an integrated approach to estimate the local scour depth around piers and abutments, collectively termed bridge foundation. Mowafy, M. H. (1997) studied experimentally local scour around pile piers. He developed two empirical equations to estimate the live local scour around pile piers. Ahmed, F. and Rajaratnam, N. (1998) studded experimentally the effect of bed roughens on flow around piers. Melville, B. W. and Chiew, Y. M. (1999) developed an empirical formula to estimate an equilibrium time scale for local scour around piers.

Framework for analysis of local scour

From the experimental observation, the equilibrium of local scour d_s around piers is a function in the following parameters:
ρ: fluid density (ML^{-3}), ν : kinematics viscosity (L^2T^{-1}), v: mean flow velocity ($L.T^{-1}$), h_1: upstream water depth (L), h_2: downstream water depth (L), D: pier diameter or width (L), b: bridge vent(L), g: gravitational acceleration ($L.T^{-2}$), sh: shape and alignment of piers, d_{85} : diameter of finer 85% from soil tested sample; and S: space between piers in longitudinal direction. The above parameters can be written as follows;

$$d_s = \phi_1(\rho, \nu, g, v, h_1, h_2, D, b, sh, S, d_{85}) \tag{1}$$

By dimensional analysis, equation 1 can be written as follows;

$$\frac{d_s}{D} = \phi_2\left(\frac{v.D}{\nu}, \frac{v^2}{gh_1}, \frac{h_1}{D}, \frac{h_2}{D}, \frac{h_3}{D}, \frac{S}{D}, \frac{d_{85}}{D} sh\right) \tag{2}$$

The dimensionless parameters have been evaluated from laboratory data and can be written as follows;

$$\frac{d_s}{D} = \phi_3(C_1, C_2, C_3, C_4, C_5, C_6, C_7, C_8) \tag{3}$$

Experimental work

Figure 1 shows schematic diagram to the experimental model. The experiments were conducted in a mobile bed flume of recirculating type and the flow system is a closed loop one. The flume dimensions are 3.70 m overall length, 0.61 m width, and

0.85 m depth. The flume is divided into three parts the inlet part, the working section and the outlet part. The dimensions of the working section are 2.10m length, 0.61m width and 0.85m total depth. The dimensions of the working section of the flume are adjusted to suite the aimed study. The flume width is reduced to 0.40 m. Intermediate piers of 4 cm width or 12cm diameter are fixed on the flume bed. The second pier is fixed after a space equal 0, 0.5D, D, 2D, 4D, 8D, 16D and 32 D from the upstream pier in the longitudinal section. The experimental program used rectangular pier with round upstream and down stream face and circular pier. The two types of piers have equal perimeter. Photos 1, 2, and 3 shows sample from tested cases. Figure 2 shows the sieve analysis of the tested sample. The figure indicated that d_{10}, d_{50}, and d_{85} equal 0.3mm, 0.5mm, and 0.80mm respectively.

Photo (1) Scour holes around two circular Piers

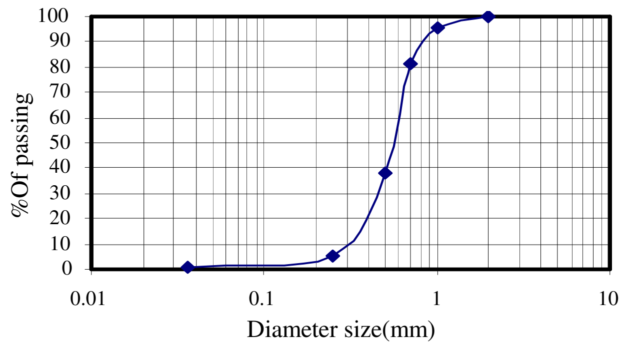

Figure(2) Sieve analysis for tested sample

Photo (2) Scour holes around rectangular pier in U.S. with circular pier in D.S.

Photo (3) Scour holes around circular pier in U.S, with Rect. pier in D.S.

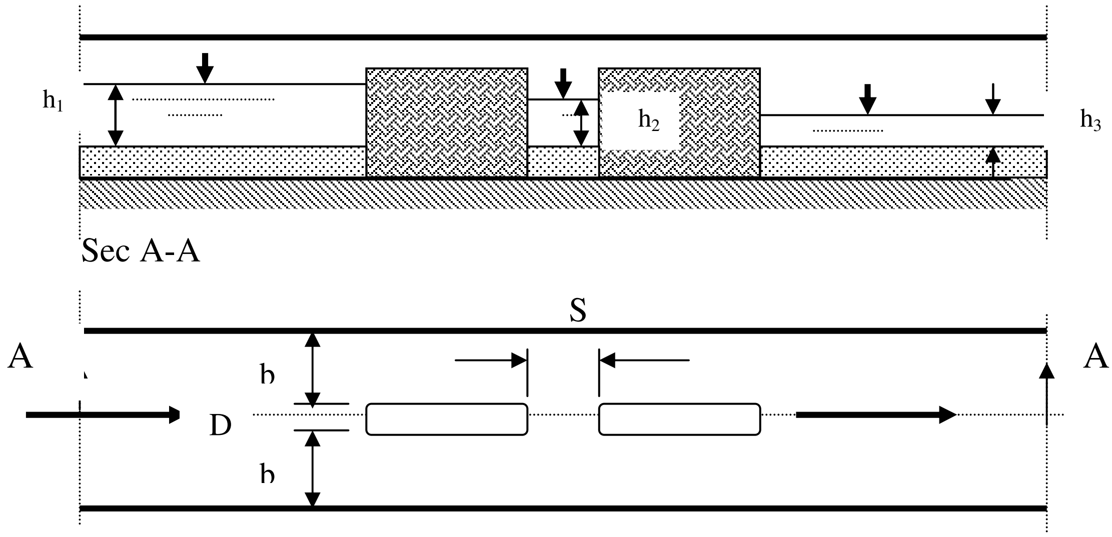

Figure 1. Alignment of experimental work

Results analysis

Effect of Space between Piers on Maximum Scour Depth

A-Rectangular Shape with Round Upstream and Downstream Face

Figures 3 to 10 show the relationship between the maximum scour depth relative to the pier width and the Froude number for the d_{85}. Figures 3 and 4 show that no scour occurred around the downstream pier for S equal 0, and 0.5D. Figures 5 to 10 show that the scour depth around the downstream pier increases as the space between the two piers increases until S equal 32D, the maximum scour depth around the upstream and downstream piers is nearly the same. In this case it is preferred that the space between the upstream and downstream piers has to be very small to give minimum scour depth.

B- Circular Piers in Upstream and Downstream

Figures 11 to 16 show the relationship between $d_{s(max)}/D$ versus Fd_{85} of using circular piers in upstream and downstream. The figures indicated that the difference between the maximum scour depth is small for S equals 0.0 and 0.5D.

For S equals D and 2D the scour depth around the downstream pier decreases and the average difference from the maximum scour increases. Figures 13 to 16 show that the maximum scour depth around the downstream pier starts to increase as the space between both two-piers increases. For S equal 8D the maximum scour depth around both the upstream and downstream piers is nearly the same. In this case it's the preferred space between the two piers (S=8D).

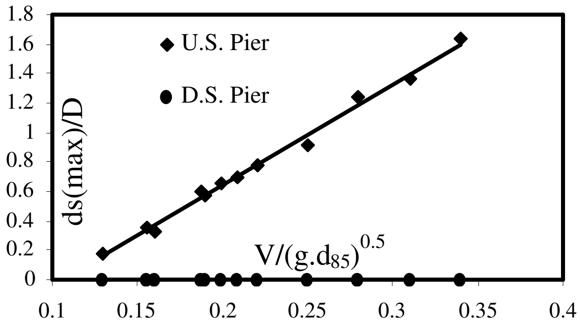

Figure(3) relationship between ds(max)/D versus $V/(g.d_{85})^{0.5}$, S=0.0

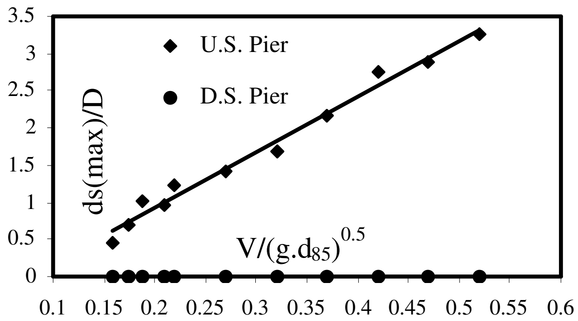

Figure(4) relationship between ds(max)/D versus $V/(g.d_{85})^{0.5}$,S=0.5D

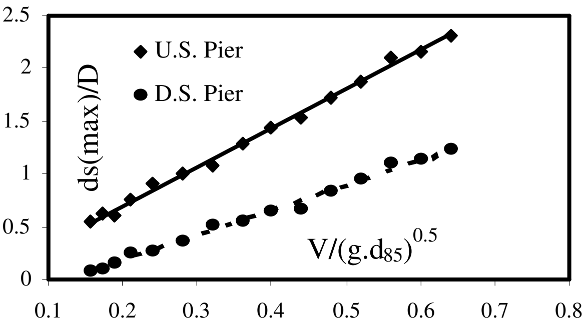

Figure(5) relationship between ds(max)/D versus $V/(g.d_{85})^{0.5}$, S=D

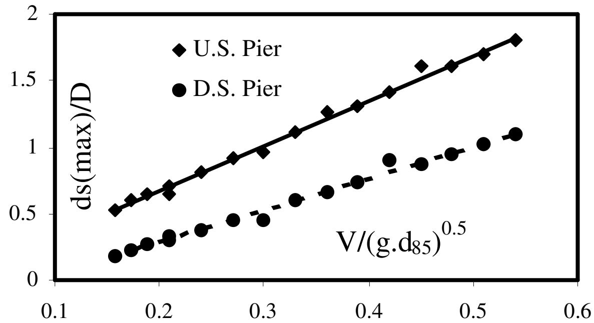

Figure(6) relationship between ds(max)/D versus $V/(g.d_{85})^{0.5}$,S=2D

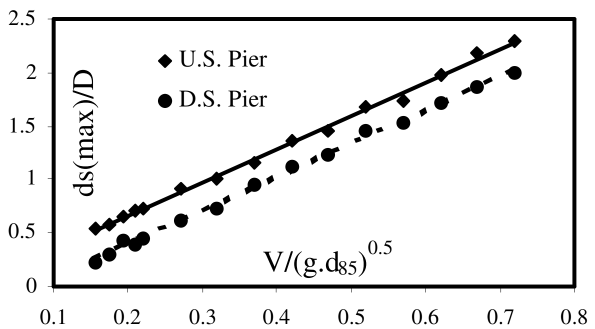

Figure(7) relationship between ds(max)/D versus $V/(g.d_{85})^{0.5}$, S=4D

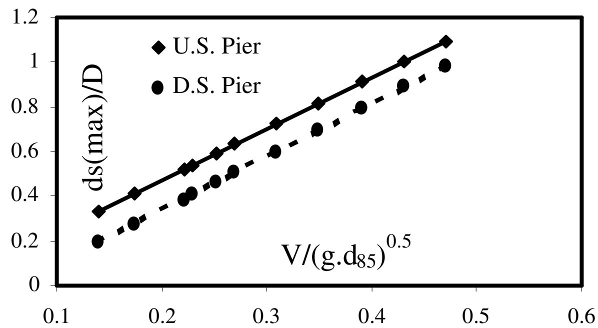

Figure(8) relationship between ds(max)/D versus $V/(g.d_{85})^{0.5}$, S=8D

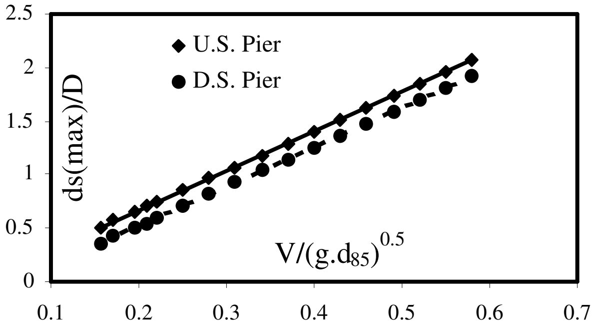

Figure(9) relationship between ds(max)/D versus $V/(g.d_{85})^{0.5}$, S=16D

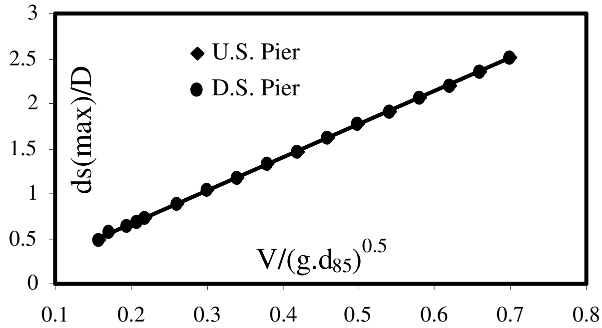

Figure(10) relationship between ds(max)/D versus $V/(g.d_{85})^{0.5}$, S=32D

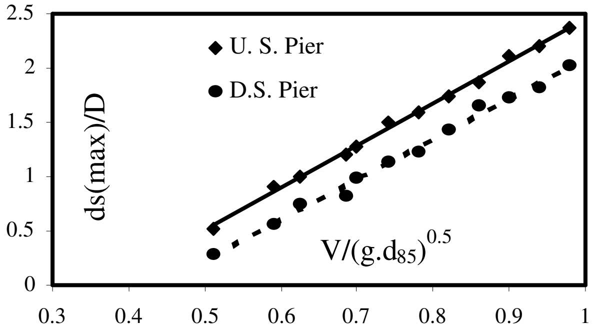

Figure(11) relationship between ds(max)/D versus $V/(g.d_{85})^{0.5}$, S=0.0

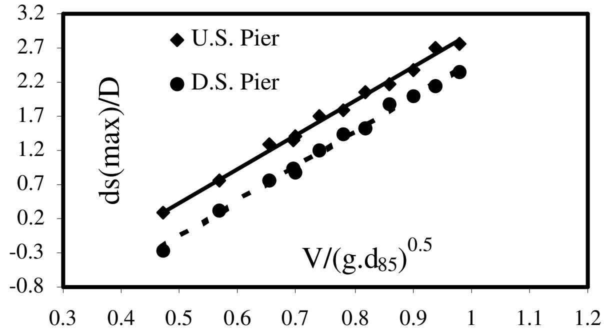

Figure(12) relationship between ds(max)/D versus $V/(g.d_{85})^{0.5}$, S=0.5D

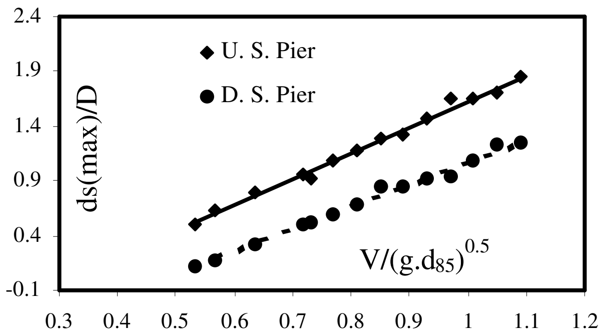

Figure(13) relationship between ds(max)/D versus $V/(g.d_{85})^{0.5}$, S=D

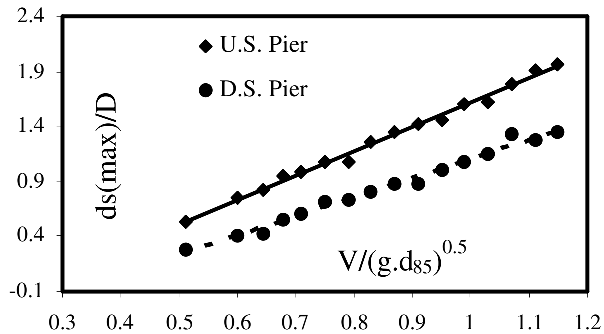

Figure(14) relationship between ds(max)/D versus $V/(g.d_{85})^{0.5}$, S=2D

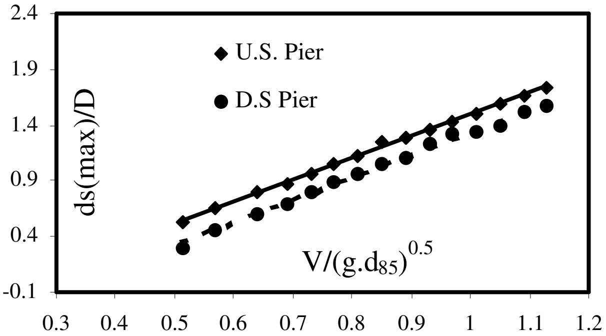

Figure(15) relationship between ds(max)/D versus $V/(g.d_{85})^{0.5}$, S=4D

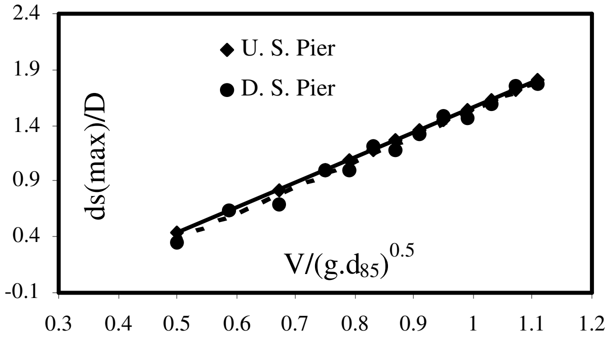

Figure(16) relationship between ds(max)/D versus $V/(g.d_{85})^{0.5}$, S=8D

C- Circular Pier in Upstream and Rectangular Pier Shape with round in downstream

Figures (17 to 20) show the effect of space between upstream circular pier and downstream rectangular pier on the maximum scour depth. The figures indicated that the scour depth around the downstream pier is large when it's close to the upstream one. Figure 20 shows that the maximum scour depth around the downstream rectangular pier is less than the maximum scour depth around the upstream circular one. In this case it is preferred to increase the distance between the upstream and downstream pier to avoid the maximum scour depth around the downstream pier.

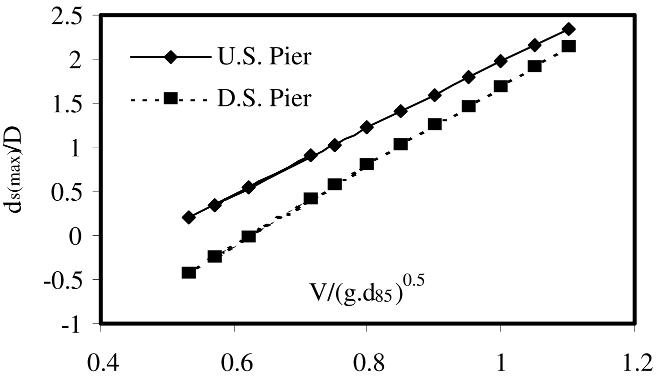

Figure(17) Relationship between ds(max)/D and $V/(g.d_{85})^{0.5}$ for upstream circular pier and downstream round rectangular pier, S=0.0

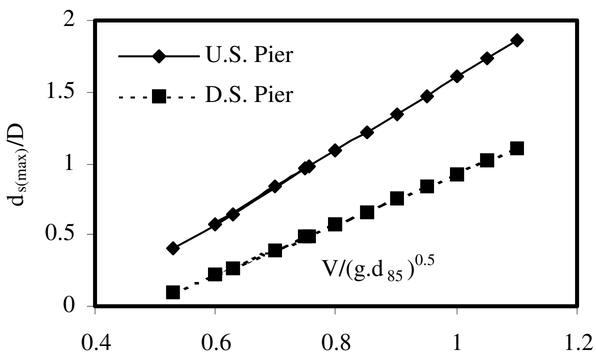

Figure(18) Relationship between ds(max)/D and $V/(g.d_{85})^{0.5}$ for upstream circular pier and downstream round rectangular pier, S=D

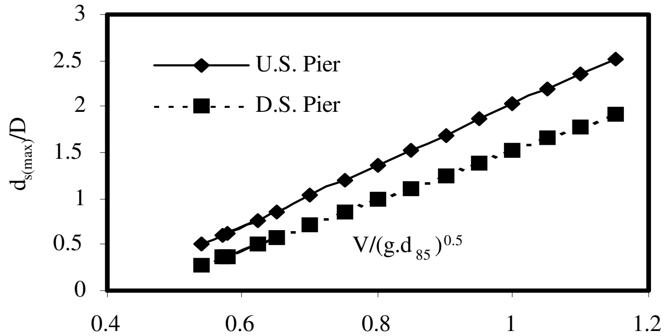

Figure(19) Relationship between ds(max)/D and $V/(g.d_{85})^{0.5}$ for upstream circular pier and downstream round rectangular pier, S= 4D

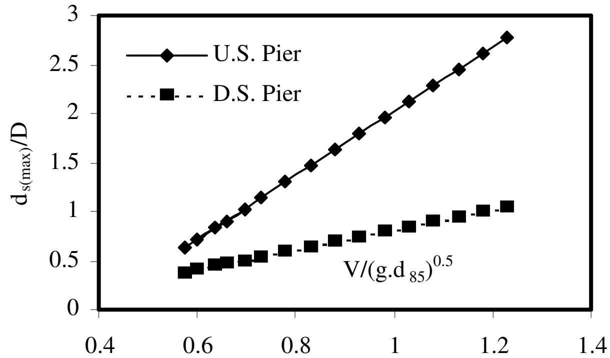

Figure(20) Relationship between ds(max)/D and $V/(g.d_{85})^{0.5}$ for upstream circular pier and downstream round rectangular pier, S= 8D

d- Rectangular Pier with Round in Upstream and Circular Pier in downstream

Figures 21 to 24 show the relationship between $d_{s(max)}/D$ versus $V/(g.d_{85})^{0.5}$ for an upstream rectangular pier and a downstream circular pier for different spaces between the two piers which equal 0, 2D, 4D and 8D. The figures indicated that for all cases the maximum scour depth around the downstream circular pier is larger than the maximum scour hole around the upstream rectangular pier with round. This means that it's preferred to choose a rectangular pier in the downstream.

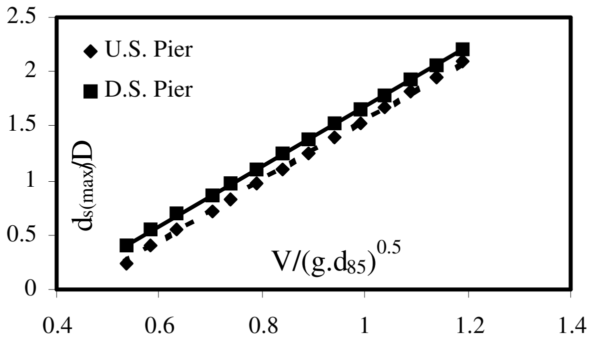

Figure(21) Relationship between ds(max)/D and $V/(g.d_{85})^{0.5}$ for upstream round rectangular pier and downstream circular pier, S=0.0

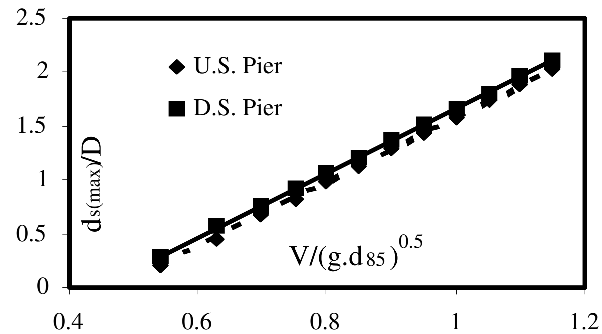

Figure(22) Relationship between ds(max)/D and $V/(g.d_{85})^{0.5}$ for upstream round rectangular pier and downstream circular pier, S= 2D

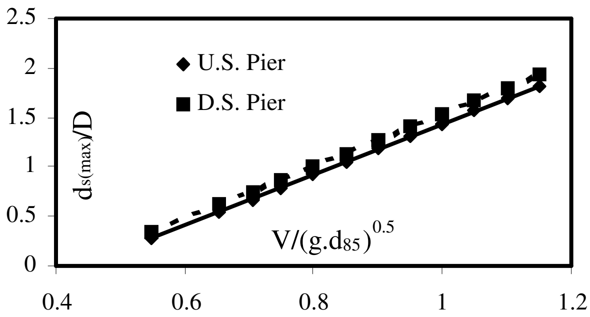

Figure(23) Relationship between ds(max)/D and V/(g.d85)$^{0.5}$ for upstream round rectangular pier and downstream circular pier, S=4D

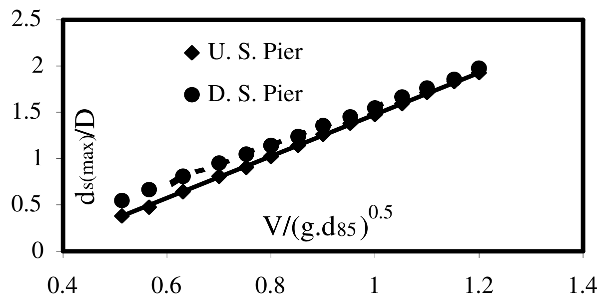

Figure(24) Relationship between ds(max)/D and V/(g.d 85)$^{0.5}$ for upstream round rectangular pier and downstream circular pier, S= 8D

e- Relationship between $d_{s(max)}$/D and V/(g.d$_{85}$)$^{0.5}$ for various spaces S for rectangular piers with round in upstream and downstream

Figure 25 shows the maximum scour depth around the upstream rectangular pier at different spaces relative to the width of the pier. The figure indicated that the maximum scour depth decreases as the space increases until S=8D. The maximum scour depth starts to increase at S=16D, 32D, and 64D. The maximum scour depth at S=64D is nearly the same as the maximum scour depth for only one pier.

Figure 26 shows the maximum scour depth around downstream rectangular pier. This figure indicated that the maximum scour depth decreases as the space between the two piers increases until S equal 8D. After that the maximum scour depth starts to increase as the space between the two piers increases until S equals 64D. Then the maximum scour depth around the downstream pier is nearly the same as the maximum scour depth around the upstream pier. The experimental work proved that the minimum scour depth around the upstream pier occurred with space equals 8D between the two piers and around the downstream pier occurred with space equals 0.0 and 0.5D between the two piers.

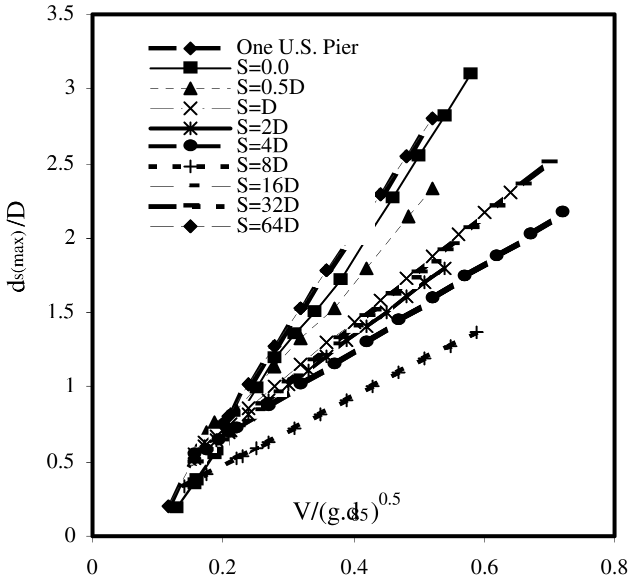

Figure(25) Relationship between $ds(max)/D$ and $V/(g.d_{85})^{0.5}$ for upstream pier, rectangular shape

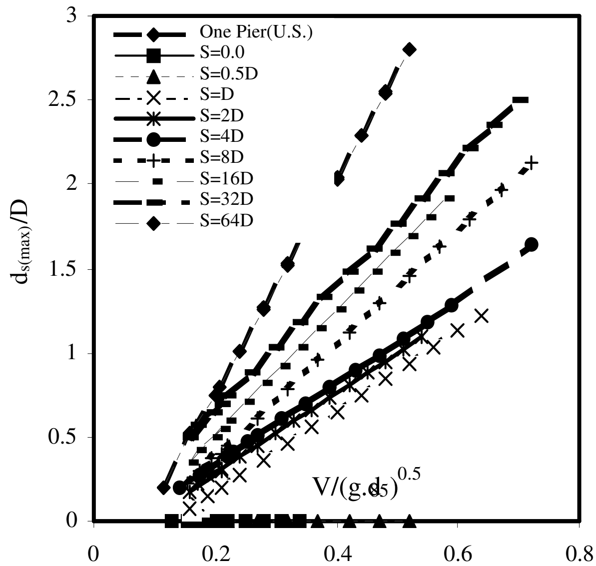

Figure(26) Relationship between $ds(max)/D$ and $V/(g.d_{85})^{0.5}$ for downstream pier, rectangular shap

f- Relationship between $d_{s(max)}/D$ and $V/(g.d_{85})^{0.5}$ for various space S in circular piers

Figure 27 shows the maximum scour depth around an upstream circular pier. The figure indicated that the maximum scour depth occurred with the space between the two piers equals 0 and 0.5D. The minimum scour depth occurred at space equal to 8D.

Figure 28 shows the scour depth around the downstream circular pier with different spaces. The scour depth increases as the space increases. The maximum scour depth occurred at space equals 16D. The minimum scour depth occurred at space equals 0.0 and 0.5D. It is preferred that the space between the upstream and the downstream circular pier is 0.0 and 0.5D.

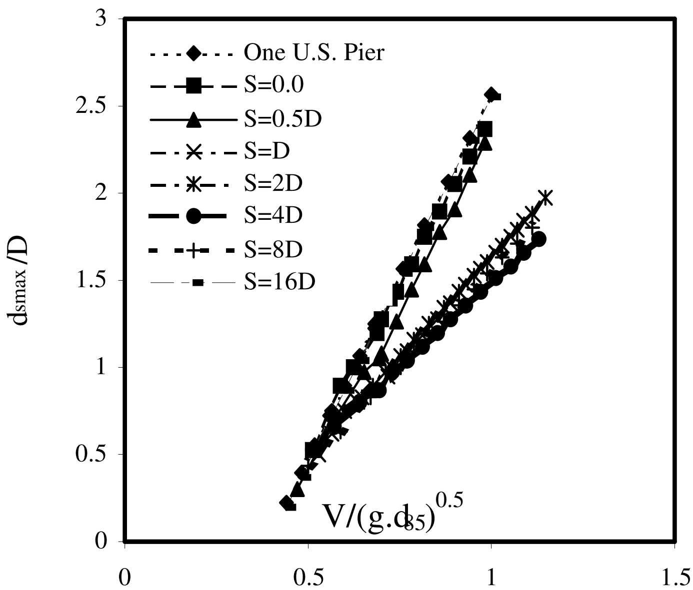

Figure(27) Relationship between $d_{s(max)}/D$ and $V/(g.d_{85})^{0.5}$ for upstream pier, circular shape

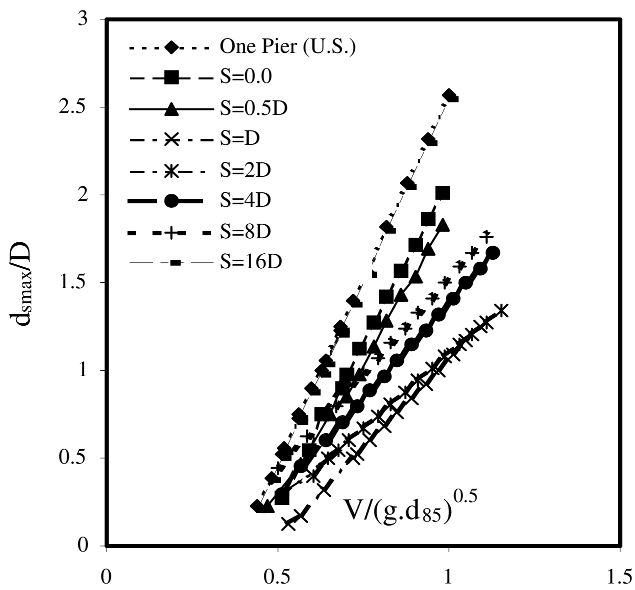

Figure(28) Relationship between $d_{s(max)}$ /D and $V/(g.d_{85})^{0.5}$ for downstream pier, circular shape

Conclusions

The maximum scour depth around both upstream and downstream piers is studied experimentally to predict the optimum space between the two piers, which gives minimum scour depth. Rectangular pier in upstream and downstream, circular pier in upstream and downstream, upstream circular pier with downstream rectangular pier, and upstream rectangular pier with downstream circular pier were studied. The main conclusions can be summarized as follows;

1- The optimum space between the two upstream and downstream rectangular shapes with round is zero which gives minimum scour depth around the downstream pier. The maximum scour depth increases as the space increases until it becomes the same as the upstream scour depth at S equal 32 D.

2- The optimum space between the two circular piers which give minimum scour depth equals D and it increases as the space increases until S equal 8D, it becomes the same as the upstream scour depth.

3- For upstream circular pier and downstream rectangular pier with round, the maximum scour hole around the upstream circular pier is larger than the maximum scour hole around the downstream rectangular with round.

4- It's preferred to use a rectangular pier with round in downstream the existing pier with space equals zero to avoided the occurrence of maximum local scour around its downstream pier.

5- If the layout of the downstream bridge prevents the space to equal zero we advise to construct apparent pier between the upstream and downstream piers to avoid the occurrence of maximum scour.

References

Ahmed, F. and Rajaratnam, N., (1998). "Flow around Bridge Piers." Journal of Hydraulic Engineering, Vol. 124, No. 3, March.

Chiew, Y. W. and Melville, B. W., (1987). "Local Scour around Bridge Piers." Journal of Hydraulic Research, Vol. 25, No. 1.

Chiew, Y. M., (1992). "Scour Protection at Bridge Piers." Journal of Hydraulic Engineering, Vol. 118, No. 9, September.

Chiew, Y. M., (1995). "Mechanics of Riprap Failure at Bridge Piers." Journal of Hydraulic Engineering, Vol. 121, No. 9, September.

Farhoud, J. and Smith, K. V. H., (1982). "Time Scale for Scour Downstream of Hydraulic Jump." Journal of Hydraulic Engineering, Vol. 108, No. HY10, October.

Johanson, P. A., (1995). "Comparison of Pier-Scour Equation Using Field Data." Journal of Hydraulic Engineering, Vol. 121, No. 8, August.

Kothyari, U. C., Garde, R. J., and Ranga Raju, K. G., (1992). "Live-Bed Scour around Cylindrical Piers." Journal of Hydraulic Research, Vol. 30, No. 5.

Mason, P. J., (1989). "Effects of Air Entrainment on Plunge Pool Scour." Journal of Hydraulic Engineering, Vol. 115, No. 3, March.

Mowafy, M. H., (1997). "Local Scour around Pile Bridge Piers." Sci. Bull. Faculty of Engineering, Ain Shams University, Vol. 32, No. 4, December.

Melville, B. W. and Raudkivi, A. J., (1996). "Effects of Foundation Geometry on Bridge Pier Scour." Journal of Hydraulic Engineering, Vol. 122, No. 4, April.

Melville, B. W. and Sutherland, A. J., (1989). "Design Method for Local Scour at Bridge Piers." Journal of Hydraulic Engineering. Vol. 120, No. 5, May.

Melville, B. W., (1997). "Pier and Abutment Scour: Integrated Approach." Journal of Hydraulic Engineering, Vol. 123, No. 2, February.

Melville, B. W. and Chiew, Y. M., (1999). "Time Scale for Local Scour at Bridge Piers." Journal of Hydraulic Engineering, Vol. 125, No. 1, January.

Uyumaz, A., (1988). "Scour Downstream of Vertical Gate." Journal of Hydraulic Engineering, Vol. 114, No. 7, July.

Notations

b : bridge vent width;
D : pier diameter or width;
d_{85} : diameter of finer 85% from soil tested sample;
g : gravitational acceleration;
h_1 : upstream water dept;
h_2 : head between two piers;
h_3 : downstream water depth;
S : space between piers in longitudinal direction.
v : mean flow velocity;
ρ : fluid density;
ϕ : functional symbol;
ν : kinematics viscosity; and
sh : shape and alignment of pier.
U. S. : upstream
D. S. : downstream